Update on the Diagnostic System

The diagnostic systems in an accelerator facility are crucial for the routine operation and improved performance of a light source. Major upgrades of the diagnostic systems are being undertaken to optimize performance and enhance the functionality of the accelerator facilities. This report provides details on these upgrades for the injector, the transport line and the storage ring.

Screen monitors of the booster, storage ring, and transport line have been upgraded by adding IEEE-1394 digital cameras. The new cameras offer higher resolution, higher sensitivity, the absence of a frame grabber, the possibility of triggering with a programmable exposure time control shutter, and radiation hardness similar to that of analogue CCDs. The beam profile is digitized in the camera. Cameras are linked via IEEE-1394A copper and IEEE-1394B fiber link to the beam profile server computer. All cameras are externally triggered by the extraction timing of the booster synchrotron. The exposure time of the camera can be adjusted according to the beam intensity to prevent saturation of the camera. Multiple exposures are supported to measure the low beam current (single bunch). The beam image is analysed using Matlab scripts. The emittance of the extracted beam of the booster is measured by the quadrupole scan method. With a well-centered beam, the beam size can be measured as a quadratic function of the quadrupole field strength, K. The Σ_{11}-element of the beam transfer matrix is given by the following expression:

$$\sum_{11} = A(K-B)^2 + C$$
$$= AK^2 - 2ABK + (C + AB^2)$$

with the parabolic fitting function:

$$\sum_{11} = \langle\sigma^2\rangle = A(K-B)^2 + C$$

Herein, A, B, and C, are the three 3 fitting parameters, and K is the quadrupole strength. The Twiss parameters can be obtained from these three fitting parameters. The emittance is given from the determinant of the beam matrix: $\varepsilon = \sqrt{AC} / S_{12}^2$. Figure 1 plots the measured horizontal beam size versus the quadrupole field strength. The fitted A, B, and C parameters are also determined. The fitted emittance is 238 nm-rad, which is consistent with the theoretical value.

An intensified gated CCD camera was used to measure the turn-by-turn beam profile at the synchrotron radiation port of the storage ring to study the bump closure of the injection local bump produced by four injection kickers. Figure 2 shows the beam profile of the consecutive five turns of the stored beam during the firing of the kickers. The image is spread out by around 4 mm in the horizontal direction and 1 mm in the vertical direction. The bump is not a closure bump. This diagnostic tool may be useful as a complementary tool for tuning injection kickers. The injected beam is observed using this tool, supporting the optimization of the injection conditions.

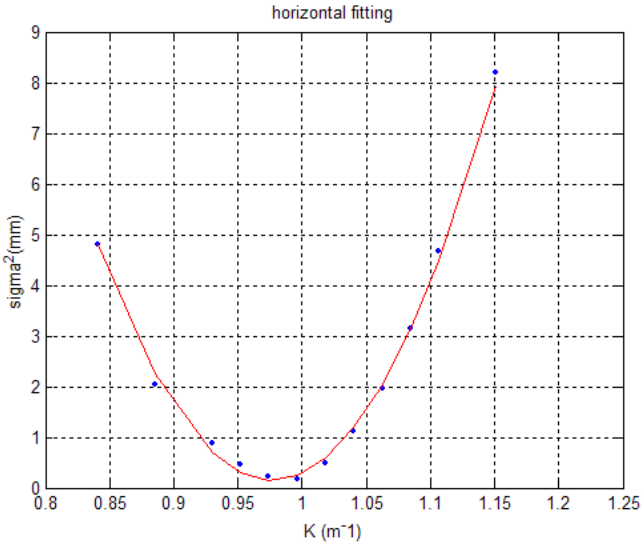

Fig. 1: Example of measuring transverse beam emittance using quadrupole scan method. Fitting parameters of A = 255.22, B = 0.98, C = 0.15, giving emittance ε_x = 238 nm-rad.

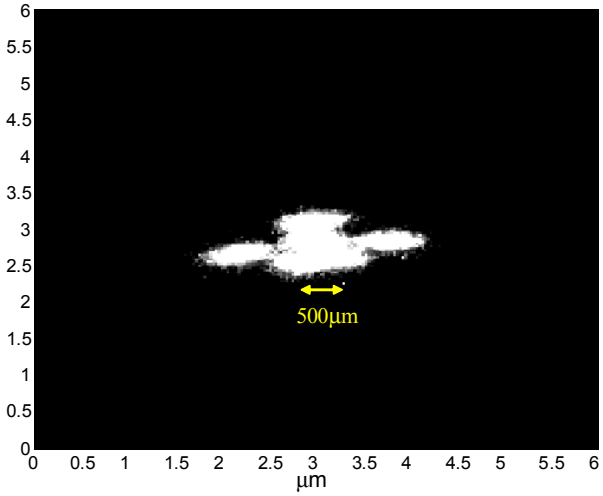

Fig. 2: The turn-by-turn beam profile of the stored beam was observed using the synchrotron light monitor. This monitor is outside the local bump formed by the injection kickers. The bump is not a closure bump.

An intensified gated CCD camera was also employed for low light observation to study the variation of the profile on a turn-by-turn basis under different operating conditions. The source point of the synchrotron radiation monitor is in the dispersion region, and energy oscillation contributes to the change in the horizontal beam size from the observed profile. If the beam is longitudinal stable, then the energy oscillation will be small; the variation in the horizontal beam size is negligible. The unstable energy oscillation caused by high order mode (HOM) of the Doris cavities is severe. The RF gap voltage modulation was used to help relieve the effect of the HOM of the Doris cavities and to stabilize the stored beam before the SRF upgrade. The modulation frequency and depth are double of the synchrotron frequency ($2f_s \approx 50$ KHz) and 5% of the total 800 KV RF gap voltage, respectively. For a single turn beam profile observation, the exposure time of the camera was set to 400 ns, which is the revolution time of the stored beam. The trigger input to the CCD camera is synchronized with the RF gap voltage modulation source. Different delay times following the trigger were observed and are shown in Fig. 3. The horizontal beam size is minimal when the RF gap voltage is minimal, and maximal when the gap voltage setting is maximal. Also the period is consistent with the modulation frequency. The horizontal beam size is stabilized using a low speed imaging system that enables the integration procedure to be performed effectively. Without this gap voltage modulation, the measured profile fluctuates indicating that the longitudinal instabilities severely degrade the quality of the beam. These

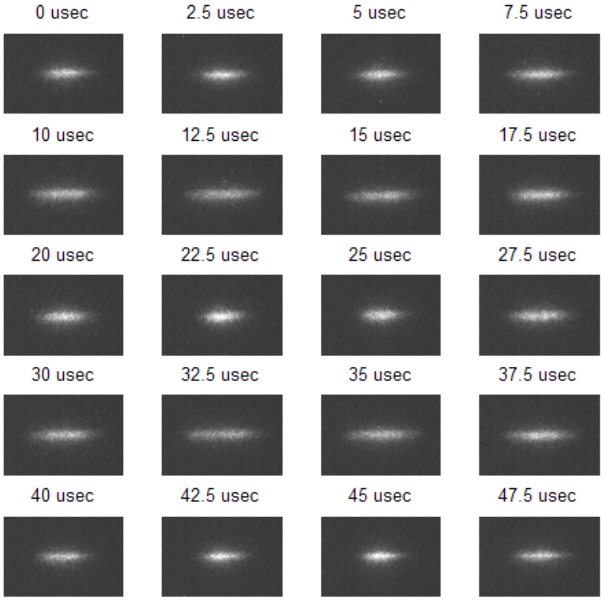

Fig. 3: Single turn beam profile observation to investigate RF gap voltage modulation effects. The image was obtained with a time delay relative to the RF gap voltage modulation signal. The period of the modulation signal is around 20 μsec.

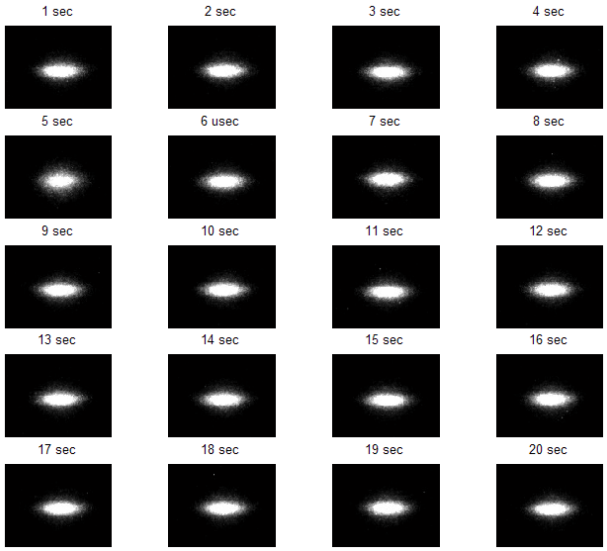

Fig. 4: Single turn profile observation for 20 sec, the storage ring operated with the SRF system. The time on the top of each profile image is the time elapsed after the beginning of image acquisition.

two Doris cavities were replaced with one CESR superconducting RF cavity to improve the stability of the beam and to double the maximum stored beam current. The measured beam profile of the single turn beam profile is much more stable than before as shown in Fig. 4. The variation of the horizontal beam size caused by the longitudinal coupled bunch oscillation is much less than for the Doris cavities, because the SRF cavity is almost HOM free.

Time domain diagnostics with transient capability are elegant tools for investigating multi-bunch instabilities and the turning of the multi-bunch feedback system. A transient digitizer is accompanied by the feedback electronics to record bunch-by-bunch and turn-by-turn beam signals. The digitizer acquired data from the transverse bunch oscillation detector and the longitudinal bunch phase detector. The CompuScope 82G digitizer was chosen because it provides a friendly application development environment (SDK for LabVIEW and MATLAB). Simple MATLAB scripts access the transient digitizer hardware to enable capture data and facilitated the integration of the analysis scripts. The trigger signal can be accompanied with the feedback Off/On to capture the transient signal for all bunches without decimation. The acquired data may have to be further reduced. Fourier analysis is performed on the acquired data to yield a high-resolution pseudospectrum. The pseudospectrum is the beam spectrum without revolution harmonics, calculated from digitized data. Figure 5 shows the typical beam pseudospectrum for RF gap voltage modulation between On and Off. The sharp peak near 190 MHz is related to one of the HOMs of the Doris cavity. The 2nd plunger of the Doris RF cavity is tuned to maintain the magnitude of this peak as stable as

possible. The RF gap voltage modulation will further reduce the strength of the instability to provide stable beams. Following the SRF upgrade, the beam spectrum is much cleaner than before. However, residual transverse and longitudinal in-stabilities remain. The transverse instabilities are much more severe because the bunch charge density is much higher after the SRF upgrade. A transverse feedback system must be used to eliminate those instabilities. Figure 6 shows beam pseudospectrum with and without a transverse feedback loop. The spectrum is clean when the feedback is applied.

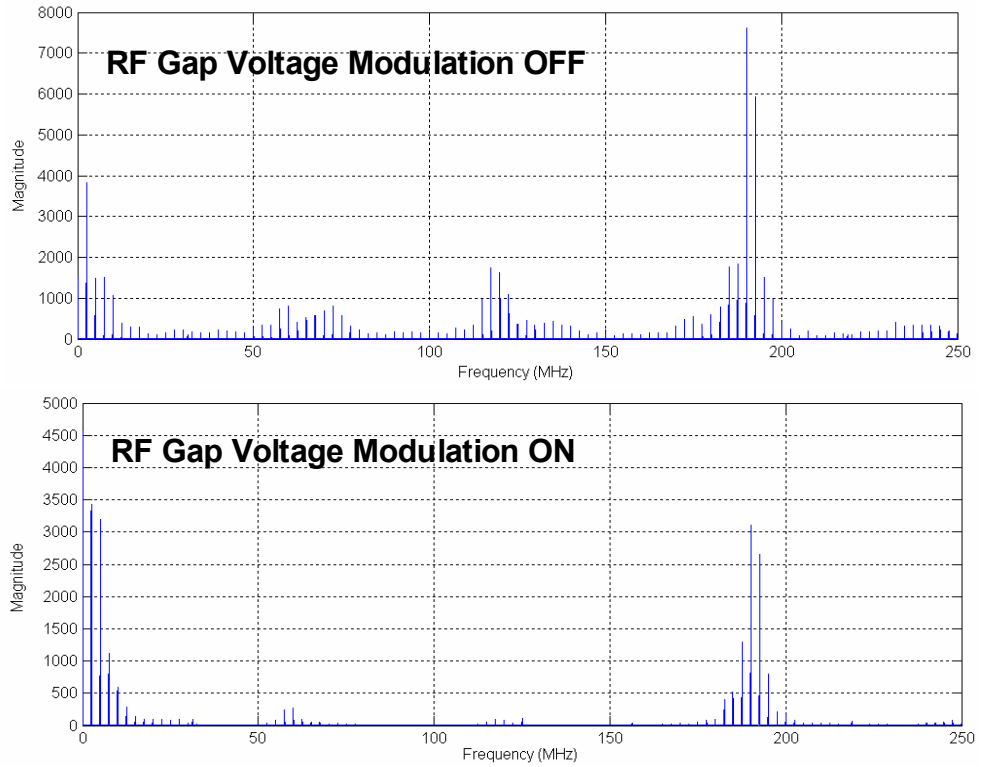

Fig. 5: Longitudinal pseudospectrum of the stored beam with/without RF gap voltage modulation.

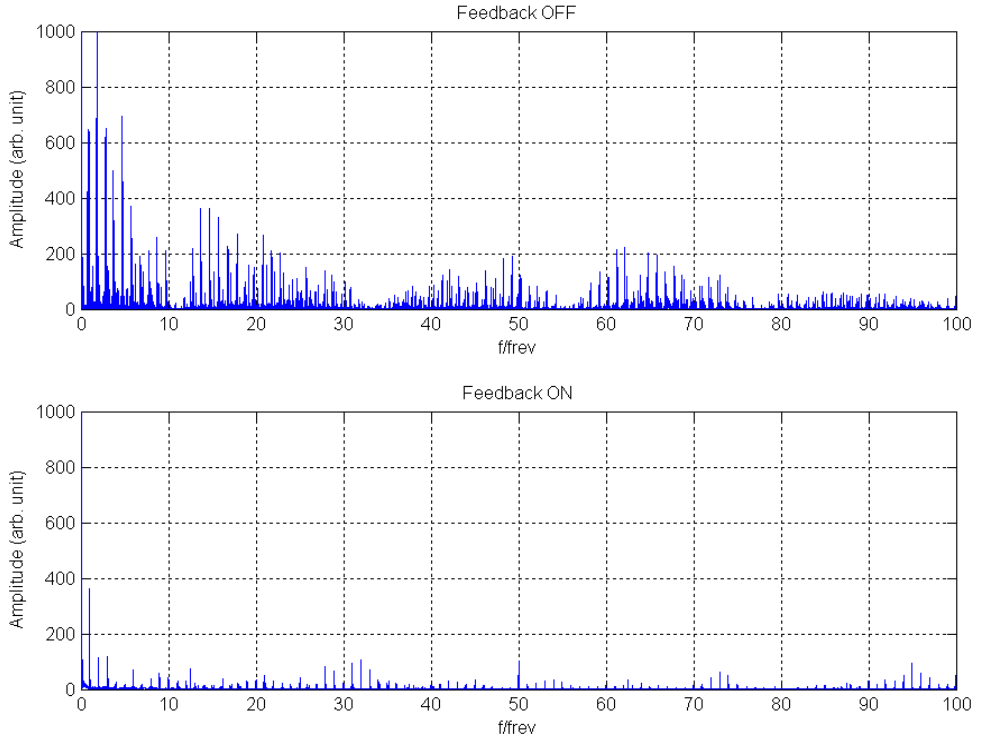

Fig. 6: Transverse pseudospectrum of the stored beam with/without transverse feedback loop.

Over the last few years, several log-ratio BPMs have been installed to measure the turn-by-turn beam position to support various studies including tune variation, nonlinear detuning, resonance, and injection. Accordingly, the functionality of the storage ring BPM system can be improved. These log-ratio BPMs are only for measuring turn-by-turn beam positions. A new generation of digital BPMs will be integrated in the existing system to improve its functionality. New BPM electronics are multi-mode and will support turn-by-turn, sub-micron beam position, as well as tune monitoring. The control system will support all kinds of software and thus support the operation of the digital BPM. The features of the new BPM system include analog multiplexing BPMs and digital BPMs, which are transparent to the users, because of the seamless integration. Figure 7 shows the typical beam

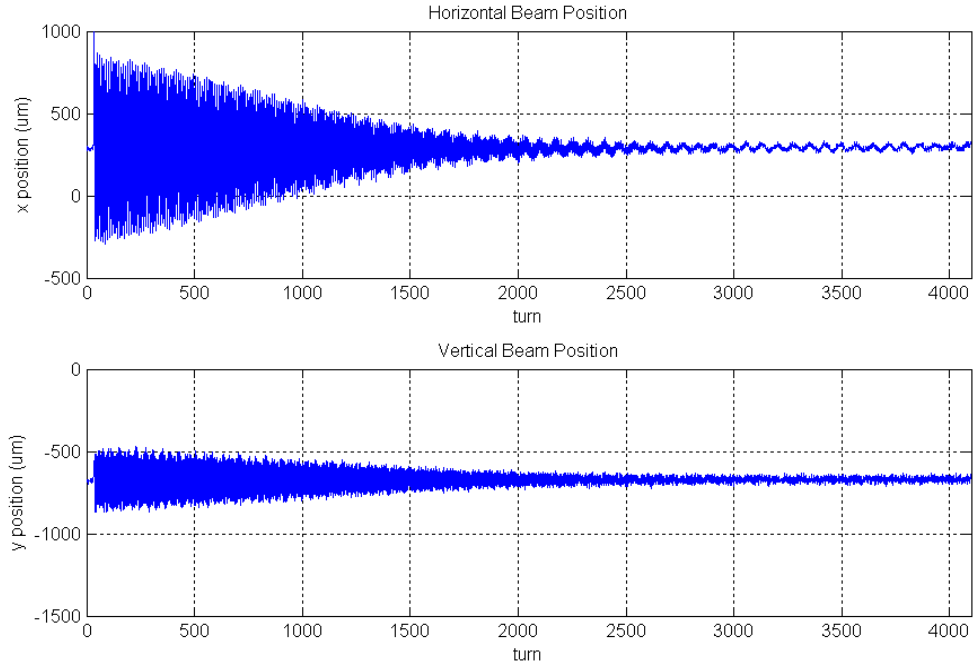

Fig. 7: Turn-by-turn beam position measured using the new digital BPM. The upper figure presents the horizontal beam position, and the lower figure shows the vertical beam position.

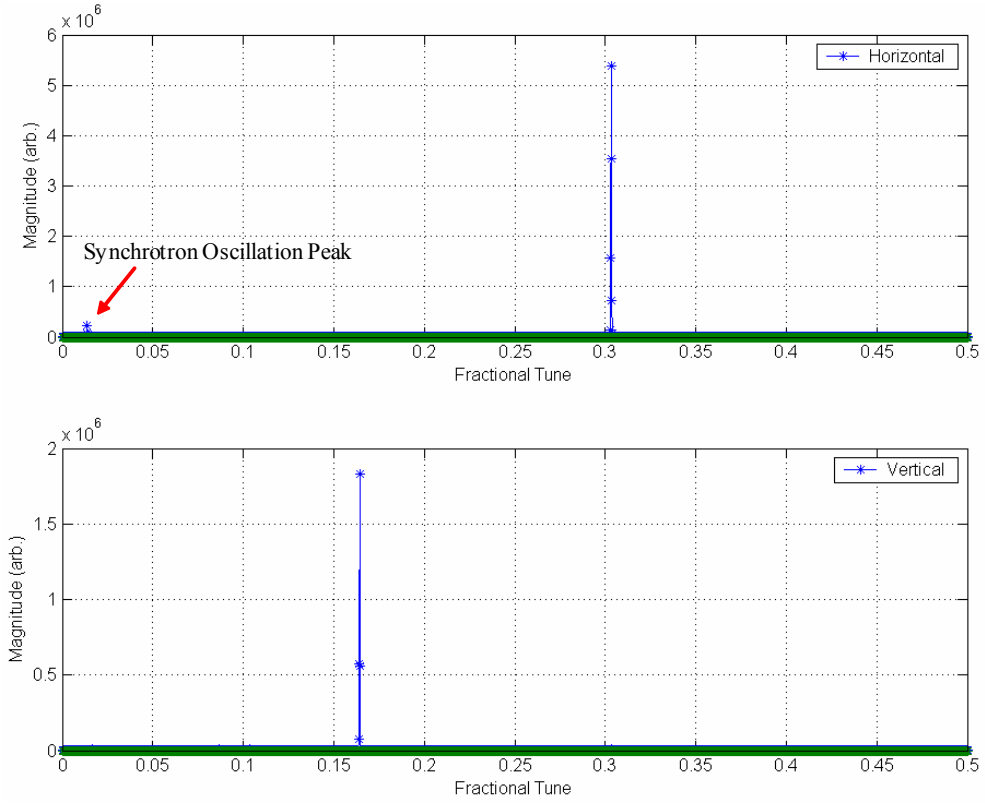

Fig. 8: Tune spectrum obtained from a Fourier analysis of the data set in Fig. 7.

position measured by a digital BPM when one of the kicker magnets is fired (K1 @ 3 KV). The upper figure depicts the damped horizontal betatron oscillation. The small regular synchrotron oscillation signal rides on the envelope of the damped oscillation, because residual longitudinal instabilities may be caused by cavities like vacuum component in the storage ring. A vertical signal is also observed following the excitation, probably because of the field imperfection of the injection kicker. Figure 8 presents the calculated tune spectrum.

Improving the performance and functionality of the diagnostic system is critical for optimizing the performance of the light source. The efforts will in a short-term focus on meeting a wide range of requirements for the operation of the machine. Advanced tools need to be developed and implemented.

AUTHORS
J. Chen, C. J. Wang, Y. T. Yang, S. Y. Hsu, C. H. Kuo, K. H. Hu, D. Lee, and K. T. Hsu
National Synchrotron Radiation Research Center, Hsinchu, Taiwan

PUBLICATIONS

- K. H. Hu, *et al.*, AIP Conf. Proc., **732**, 302 (2004) 302.
- C. J. Wang, *et al.*, AIP Conf. Proc., **732**, 462 (2004).

CONTACT E-MAIL
kuotung@nsrrc.org.tw